

# Internal and net roof pressures for a dynamically flexible building with a dominant wall opening

Rajnish N Sharma\*

*Department of Mechanical Engineering, The University of Auckland,  
Private Bag 92019, Auckland, New Zealand*

*(Received July 29, 2011, Revised February 27, 2011, Accepted March 12, 2012)*

**Abstract.** This paper describes a study of the influence of a dynamically flexible building structure on pressures inside and net pressures on the roof of low-rise buildings with a dominant opening. It is shown that dynamic interaction between the flexible roof and the internal pressure results in a coupled system that is similar to a two-degree-of-freedom mechanical system consisting of two mass-spring-damper systems with excitation forces acting on both the masses. Two resonant modes are present, the natural frequencies of which can readily be obtained from the model. As observed with quasi-static building flexibility, the effect of increased dynamic flexibility is to reduce the first natural frequency as well as the corresponding peak value of the admittance, the latter being the result of increased damping effects. Consequently, it is found that the internal and net roof pressure fluctuations (RMS coefficients) are also reduced with dynamic flexibility. This model has been validated from experiments conducted using a cylindrical model with a leeward end flexible diaphragm, whereby good match between predicted and measured natural frequencies, and trends in peak admittances and RMS responses with flexibility, were obtained. Furthermore, since significant differences exist between internal and net roof pressure responses obtained from the dynamic flexibility model and those obtained from the quasi-static flexibility model, it is concluded that the quasi-static flexibility assumption may not be applicable to dynamically flexible buildings. Additionally, since sensitivity analyses reveal that the responses are sensitive to both the opening loss coefficient and the roof damping ratio, careful estimates should therefore be made to these parameters first, if predictions from such models are to have significance to real buildings.

**Keywords:** internal pressure; dominant opening; dynamic flexibility; flexible roof; net roof pressure; helmholtz resonance

---

## 1. Introduction

The significant influence that building internal pressure can have on the safety of buildings and structures during windstorms is well recognised. This is reflected firstly from regular research interests over the decades and secondly from the internal pressure provisions of wind loading codes (Standards Australia/Standards New Zealand, 2002; American Society of Civil Engineers, 2005). The limiting case of internal pressure in a rigid, non-porous, single compartment building with a single dominant opening has been thoroughly studied (Holmes 1979, Liu and Saathoff 1981,

---

\*Corresponding author, Professor, E-mail: [r.sharma@auckland.ac.nz](mailto:r.sharma@auckland.ac.nz)

Vickery and Bloxham 1992, Vickery 1994, Sharma and Richards 1997a, Sharma and Richards 2003, Ginger *et al.* 2008 and Sharma *et al.* 2010, amongst others). However, real buildings can be flexible except when constructed from rigid concrete (Vickery 1986, Sharma 2008), are porous due to tolerances around fittings or due to provision of ventilation pathways (Oh *et al.* 2007), and are internally compartmentalised (Sharma 2003). While the ideal treatment of a rigid, non-porous, single compartment building with a single dominant opening provides great insight into the limiting characteristics of building internal pressure, from a design viewpoint however, it is imperative that the influence of envelope flexibility, porosity, and compartmentalisation be understood.

The influence of the flexibility of the envelope on internal pressure developed inside relatively small residential and light commercial buildings has received relatively little attention in the past. Vickery (1986) assumed the building structure to respond in a quasi-static manner (i.e., where deflections are assumed to be proportional to the applied load at all times) and proposed the idea of an effective volume  $\nabla_e$  to model the influence of building flexibility on the response of internal pressure

$$\frac{\rho L_e \nabla_e}{\gamma A_o p_a} \ddot{C}_{pi} + \frac{C_L \rho q \nabla_e^2}{2(\gamma A_o p_a)^2} |\dot{C}_{pi}| \dot{C}_{pi} + C_{pi} = C_{pe} \quad (1)$$

In Eq. (1),  $\rho$  is the density of ambient air;  $p_a$  is the ambient pressure;  $\gamma$  is the ratio of specific heats for air;  $C_L$  is the opening loss coefficient;  $A_o$  is the opening area;  $L_e$  is the effective length of the air jet / slug at the opening used to define the inertia of the system;  $q = 0.5 \rho \bar{U}_h^2$  is the reference ridge-height dynamic pressure based on ridge-height wind velocity  $\bar{U}_h$ , and  $C_{pe} = p_e / q$  and  $C_{pi} = p_i / q$  are the (opening) area-averaged external and internal pressure coefficients respectively. The effective volume  $\nabla_e$  is defined in terms of the nominal internal volume of the building  $\nabla_o$  by

$$\nabla_e = \nabla_o (1 + b) \quad (2)$$

where

$$b = \frac{\gamma p_a}{k_b} \quad (3)$$

is the ratio of the bulk modulus of air  $\gamma p_a$  to the building bulk modulus  $k_b$  defined as the ratio of increase in net pressure loading to volumetric strain. Vickery (1986) estimated  $b$  to vary between 0.2 for stiff structures to 5.0 for flexible large span roof structures.

Vickery's study was focused upon the characteristics of internal pressure, but did not include the action of the fluctuating external pressure on the flexible envelope. Furthermore, the characteristics of net envelope pressures were not addressed. Two theoretical models, those of Novak and Kassem (1990) and Vickery and Georgiou (1991) attempted to describe the interaction between a flexible roof backed by a cavity with openings as simple two-degree-of-freedom systems. These studies were directed at large span self- or air-supported structures such as arenas

and sports stadia. The first validated the theoretical model with experimental tests on scaled models in still air, in predicting resonance frequencies and the damping ratios. Vickery and Georgiou (1991) considered the effect of the wall opening area to the roof area ratio, on the form of transfer functions and RMS values of the fluctuating roof response. The full characteristics of roof response and the net pressures were not considered in these studies. Sharma and Richards (1997b) also presented an analytical model for internal pressure dynamics with roof flexibility, but which did not include the influence of roof external pressure. Pearce and Sykes (1999) reported on wind tunnel internal pressure tests on a model-scale cavity resonator with a flexible membrane roof in the parameter range  $0.02 < b < 7.5$ . They concluded that increased flexibility of the roof membrane reduced the value of the Helmholtz frequency and also reduced the magnitude of the resonant response. This was in agreement with the deductions that can be made from the model, Eq. (1), of Vickery (1986), although the influence of roof external pressure is not accounted for in this model.

Recently, Sharma (2008) following from an earlier work (Sharma 1996) presented a general model for the response of internal pressure in any flexible building with a dominant opening

$$\frac{\rho L_e \nabla_o}{\gamma c A_o p_a} \left( \ddot{C}_{pi} - \dot{v} \dot{C}_{pi} - \frac{\gamma p_a}{q} \ddot{v} \right) + \frac{C_L \rho q \nabla_o^2}{2(\gamma A_o p_a)^2} \left| \dot{C}_{pi} + \frac{\gamma p_a}{q} \dot{v} \right| \left( \dot{C}_{pi} + \frac{\gamma p_a}{q} \dot{v} \right) + C_{pi} = C_{pe} \quad (4)$$

In Eq. (4)

$$v = \frac{\Delta \nabla}{\nabla_o} = \frac{\nabla - \nabla_o}{\nabla_o} = \frac{\nabla}{\nabla_o} - 1 \quad (5)$$

is the ratio of the change in building internal volume  $\nabla - \nabla_o$  to the nominal volume  $\nabla_o$ ;  $\nabla$  is the instantaneous physical internal volume of the building; and  $c$  is the opening contraction coefficient representing flow contraction past the opening via the formation of a vena-contracta in the air jet (Sharma and Richards 1997a). For the case of the quasi-static flexibility of the roof, Sharma (2008, 1996) represented the change in (non-dimensional) internal volume by

$$v = \frac{\nabla - \nabla_o}{\nabla_o} = \frac{q}{k_b} (C_{pi} - C_{pr}) \quad (6)$$

in which  $C_{pr}$  is the area-averaged fluctuating external roof pressure coefficient; and then derived an equation

$$\begin{aligned} & \frac{\rho L_e \nabla_o (1+b)}{\gamma c A_o p_a} \left( \ddot{C}_{pi} - \frac{b}{(1+b)} \ddot{C}_{pr} \right) \\ & + \frac{C_L \rho q \nabla_o^2 (1+b)^2}{2(\gamma A_o p_a)^2} \left| \dot{C}_{pi} - \frac{b}{(1+b)} \dot{C}_{pr} \right| \left( \dot{C}_{pi} - \frac{b}{(1+b)} \dot{C}_{pr} \right) + C_{pi} = C_{pe} \end{aligned} \quad (7)$$

which describes the response of building internal pressure to external pressures acting at a dominant opening and on the roof structure that responds in a quasi-static manner. It is different from the results obtained by Vickery (1986) because the effects of external pressure on the flexible component (i.e., the roof) have been included. The un-damped Helmholtz frequency  $f_{HH}' = \omega_{HH}' / 2\pi$  is readily obtained from Eq. (8)

$$f_{HH}' = \frac{1}{2\pi} \sqrt{\frac{\gamma c A_o P_a}{\rho L_e \nabla_o (1+b)}} = \frac{1}{2\pi} \sqrt{\frac{\gamma c A_o P_a}{\rho L_e \nabla_o}} \frac{1}{\sqrt{(1+b)}} = \frac{f_{HH}}{\sqrt{(1+b)}} \quad (8)$$

where  $f_{HH}$  is the Helmholtz frequency for a corresponding rigid building. Eq. (7) was also linearised and admittance functions were derived. Sharma (2008) combined the above model with wind tunnel testing to demonstrate that the flexibility of the building reduces fluctuations in internal and net envelope pressures, as indicated by somewhat smaller RMS pressure coefficients relative to the case of a rigid building. Furthermore, it was shown that when the roof external pressure fluctuations were accounted for, the RMS values of internal as well as net roof pressures were lowered further for the cases studied ( $b = 0.334, 1.335$ ).

The work described in the present paper is an extension of the study on quasi-static flexibility reported by Sharma (2008), to consider the influence of dynamic flexibility of the building envelope. This is a subset of a more comprehensive building internal pressure study of Sharma (1996). An extension of this work to include the additional influence of background leakage is being published separately; see Guha *et al.* (2012).

Personal experiences of the author during windstorms and other literature (e.g., Hoxey and Richards 1995) suggest that many residential and light commercial buildings and their envelopes may respond significantly, and in some instances behave in a dynamic manner. This is more common for the roof than it is for the walls because of the inherent greater flexibility of the roof on many tropical buildings. These include the portal frame and concrete wall – corrugated roofing constructions. Dynamic heaving action of the roof is not uncommon in such building construction types. An example of the portal frame building is the Silsoe Structures Building (SSB) (Hoxey and Richards 1995), and the response of its roof during a storm has been documented on video, which clearly shows the greater flexibility of its roof in comparison with the walls. Furthermore, Robertson (1992) has shown that the SSB has a frame natural frequency of 4 Hz, and for which a 1 Hz Helmholtz resonance frequency was also recorded. The concrete wall – corrugated roofing construction is common in the Pacific Island countries, like Fiji, in which the walls are extremely rigid. Lift-off of the entire roof structure in the latter building type is not uncommon. It is therefore vitally important that the effects of dynamic building flexibility on internal and net envelope pressures be properly understood.

## 2. Dynamic structural response: development of equations

If the structural frequency of the building roof (or wall(s)) is close to the expected Helmholtz frequency, then dynamic interaction between the internal pressure system and the flexible component may be expected. As discussed earlier, many low-rise buildings are more flexible in

the roof than in the walls. To gain insight into the influence of flexibility, such buildings may be modelled by a building where the volume changes are provided mostly by vertical roof deflections.

### 2.1 The dynamic building model

Consider a building of height  $H$  and roof plan area  $A_r$  as illustrated in Fig. 1.

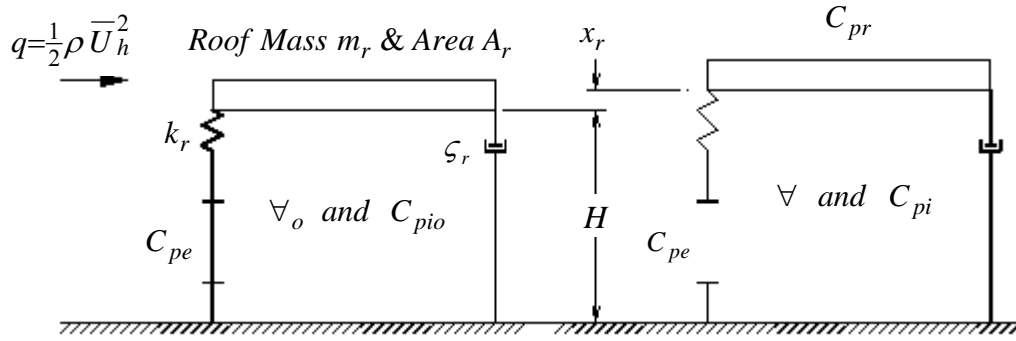


Fig. 1 The dynamic building model with a flexible roof structure

If the roof has mass  $m_r$ , a structural natural frequency  $\omega_r = 2\pi f_r$  (structural stiffness  $k_r = m_r \omega_r^2$ ) and damping ratio  $\zeta_r$  (that includes structural, acoustic, and aerodynamic damping), and it is assumed to behave linearly, then its vertical response  $x_r$  to fluctuating internal and space averaged external roof pressures  $p_r = C_{pr} \times q$  will be governed by

$$\ddot{x}_r + 2\zeta_r \omega_r \dot{x}_r + \omega_r^2 x_r = \frac{q A_r}{m_r} (C_{pi} - C_{pr}) \quad (9)$$

Since volume changes are provided by the vertical movement of the roof, the non-dimensional volume change can be expressed as

$$v = \frac{\Delta \nabla}{\nabla_o} = \frac{A_r x_r}{A_r H} = \frac{x_r}{H} \quad (10)$$

Substitution of Eq. (10) and the time derivatives of  $v$  into the equation of motion for the roof described by Eq. (9), yields the result

$$\ddot{v} + 2\zeta_r \omega_r \dot{v} + \omega_r^2 v = \frac{q A_r^2}{m_r \nabla_o} (C_{pi} - C_{pr}) \quad (11)$$

This equation can be solved simultaneously with Eq. (4) for the responses of internal pressure and the roof, to external pressures applied at the opening and the flexible roof. The determination of the admittance functions however requires a linearized approach.

## 2.2 Linearized model

Fig. 2 represents a linearized system in which an air jet / slug of mass  $m_j = \rho c A_o L_e$  oscillates at the opening with the backing of the building cavity making up a pneumatic spring system. This system has an equivalent linear damping coefficient  $c_j$  (Sharma 2008, 2011)

$$c_j = \frac{\sqrt{8\pi} c^2 C_L \rho q \nabla_o f_{HH} (2\bar{C}_{pe} I_u)}{\gamma P_a} \quad (12)$$

from which a linear damping ratio  $\zeta_j$  may be written

$$\zeta_j = \frac{c_j}{2\sqrt{m_j k_j}} = \frac{C_L c \rho \bar{U}_h^2 \nabla_o \bar{C}_{pe} I_u}{\sqrt{2\pi} \gamma A_o L_e P_a} \quad (13)$$

In this model, the roof also behaves linearly.

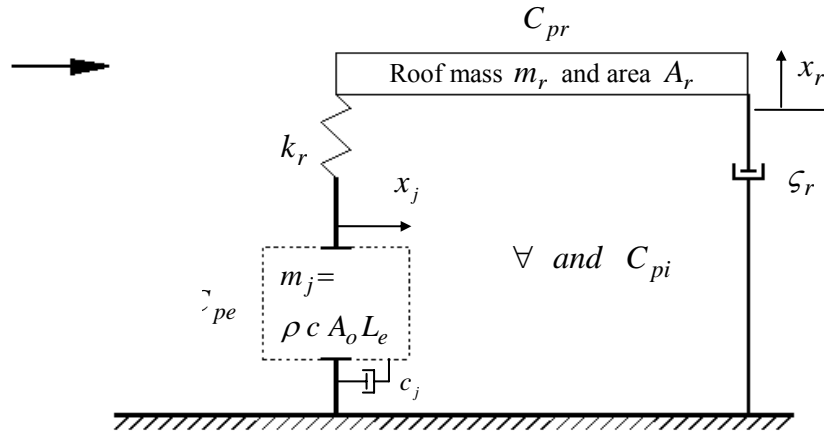


Fig. 2 Coupling of the linearized internal pressure and flexible roof systems

If the air jet and the roof are displaced by  $x_j$  and  $x_r$  respectively, then the change in internal volume is given by the difference

$$\Delta \nabla = \nabla - \nabla_o = A_r x_r - c A_o x_j \quad (14)$$

which in most cases can be assumed to be significantly smaller than the nominal volume. When this applies, then using the isentropic gas law for air, the internal pressure coefficient can be expressed in terms of the air jet and roof deflections as

$$C_{pi} = \frac{\gamma P_a}{q \nabla_o} (c A_o x_j - A_r x_r) \quad (15)$$

By summation of forces and using Eq. (15), the equations of motion for the air jet and the roof can be reduced to the following

$$\ddot{x}_j + 2\zeta_j \omega_{HH} \dot{x}_j + \omega_{HH}^2 x_j = \frac{q}{\rho_a L_e} C_{pe} + \omega_{HH}^2 \frac{A_r}{c A_o} x_r \quad (16)$$

$$\ddot{x}_r + 2\zeta_r \omega_r \dot{x}_r + (\omega_r^2 + \omega_{rp}^2) x_r = -\frac{q A_r}{m_r} C_{pr} + \omega_{rp}^2 \frac{c A_o}{A_r} x_j \quad (17)$$

where  $\omega_{HH} = \sqrt{\frac{\gamma c A_o P_a}{\rho L_e \nabla_o}} = 2\pi f_{HH}$  = angular Helmholtz frequency of the air jet-cavity system alone (i.e., for the rigid building case),

$\omega_{rp} = \sqrt{\frac{\gamma A_r^2 P_a}{m_r \nabla_o}} = 2\pi f_{rp}$  = angular frequency associated with the pneumatic stiffness of the roof with respect to the contained air, and

$$2\zeta_j \omega_{HH} = \frac{c_j}{\rho c A_o L_e}$$

In order to obtain the admittance functions, these equations are first transformed into the frequency domain leading to the final results

$$C_{pi}(j\omega) = \chi_{ie}(j\omega) \times C_{pe}(j\omega) + \chi_{ir}(j\omega) \times C_{pr}(j\omega) \quad (18)$$

$$\chi_{ie}(j\omega) = \frac{\omega_{HH}^2 ((\omega_r^2 - \omega^2) + j(2\zeta_r \omega_r \omega))}{(\omega^4 - \omega_A^2 \omega^2 + \omega_B^4) + j(\omega_C^3 \omega - \omega_D \omega^3)} = |\chi_{ie}| (\cos(\phi_{ie}) + j \sin(\phi_{ie})) \quad (19)$$

$$|\chi_{ie}| = \left( \frac{\omega_{HH}^4 ((\omega_r^2 - \omega^2)^2 + (2\zeta_r \omega_r \omega)^2)}{(\omega^4 - \omega_A^2 \omega^2 + \omega_B^4)^2 + (\omega_C^3 \omega - \omega_D \omega^3)^2} \right)^{1/2} \quad (20)$$

$$\phi_{ie} = \arctan\left(\frac{2\zeta_r \omega_r \omega}{\omega_r^2 - \omega^2}\right) - \arctan\left(\frac{\omega_C^3 \omega - \omega_D \omega^3}{\omega^4 - \omega_A^2 \omega^2 + \omega_B^4}\right) \quad (21)$$

$$\chi_{ir}(j\omega) = \frac{\omega_{rp}^2(-\omega^2 + j2\zeta_j\omega_{HH}\omega)}{(\omega^4 - \omega_A^2\omega^2 + \omega_B^4) + j(\omega_C^3\omega - \omega_D\omega^3)} = |\chi_{ir}|(\cos(\phi_{ir}) + j\sin(\phi_{ir})) \quad (22)$$

$$|\chi_{ir}| = \left( \frac{\omega_{rp}^4(\omega^4 + (2\zeta_j\omega_{HH}\omega)^2)}{(\omega^4 - \omega_A^2\omega^2 + \omega_B^4)^2 + (\omega_C^3\omega - \omega_D\omega^3)^2} \right)^{1/2} \quad (23)$$

$$\phi_{ir} = \arctan\left(\frac{-2\zeta_j\omega_{HH}}{\omega}\right) - \arctan\left(\frac{\omega_C^3\omega - \omega_D\omega^3}{\omega^4 - \omega_A^2\omega^2 + \omega_B^4}\right) \quad (24)$$

in which

$$\begin{aligned} \omega_A^2 &= \omega_r^2 + \omega_{rp}^2 + \omega_{HH}^2 + 2\zeta_r\omega_r \times 2\zeta_j\omega_{HH} = (2\pi f_A)^2 \\ \omega_B^4 &= \omega_{HH}^2\omega_r^2 = (2\pi f_B)^4 \\ \omega_C^3 &= 2\zeta_r\omega_r\omega_{HH}^2 + 2\zeta_j\omega_{HH}(\omega_r^2 + \omega_{rp}^2) = (2\pi f_C)^3 \\ \omega_D &= 2\zeta_r\omega_r + 2\zeta_j\omega_{HH} = 2\pi f_D \end{aligned}$$

The admittance functions for the internal pressure and the net roof pressure  $|\chi_{iq}|^2$  and  $|\chi_{nq}|^2$  relative to the onset ridge-height dynamic pressure are then obtained from (Sharma 2008)

$$|\chi_{iq}|^2 = \frac{S_{pi}}{S_q} \left( \frac{1}{\bar{C}_{pi}} \right)^2 = |\chi_{ie}|^2 |\chi_{eq}|^2 \left( \frac{\bar{C}_{pe}}{\bar{C}_{pi}} \right)^2 + |\chi_{ir}|^2 |\chi_{rq}|^2 \left( \frac{\bar{C}_{pr}}{\bar{C}_{pi}} \right)^2 \quad (25)$$

$$+ 2|\chi_{ie}||\chi_{eq}||\chi_{ir}||\chi_{rq}| \left( \frac{\bar{C}_{pe}}{\bar{C}_{pi}} \right) \left( \frac{\bar{C}_{pr}}{\bar{C}_{pi}} \right) \cos(\phi_{ie} - \phi_{ir} + \phi_{e/r})$$

$$\begin{aligned} |\chi_{nq}|^2 &= \frac{S_{pn}}{S_q} \left( \frac{1}{\bar{C}_{pn}} \right)^2 = |\chi_{ie}|^2 |\chi_{eq}|^2 \left( \frac{\bar{C}_{pe}}{\bar{C}_{pn}} \right)^2 + (|\chi_{ir}|^2 + 1) |\chi_{rq}|^2 \left( \frac{\bar{C}_{pr}}{\bar{C}_{pn}} \right)^2 \\ &+ 2|\chi_{ie}||\chi_{eq}||\chi_{ir}||\chi_{rq}| \left( \frac{\bar{C}_{pe}}{\bar{C}_{pn}} \right) \left( \frac{\bar{C}_{pr}}{\bar{C}_{pn}} \right) \cos(\phi_{ie} - \phi_{ir} + \phi_{e/r}) \\ &- 2|\chi_{ie}||\chi_{eq}||\chi_{rq}| \left( \frac{\bar{C}_{pe}}{\bar{C}_{pn}} \right) \left( \frac{\bar{C}_{pr}}{\bar{C}_{pn}} \right) \cos(\phi_{ie} + \phi_{e/r}) \\ &- 2|\chi_{ir}||\chi_{rq}|^2 \left( \frac{\bar{C}_{pr}}{\bar{C}_{pn}} \right)^2 \cos(\phi_{ir}) \end{aligned}$$

(26)

in which the opening external and roof external pressure admittance functions  $|\chi_{eq}|^2$  and  $|\chi_{rq}|^2$  respectively are given by

$$|\chi_{eq}|^2 = \frac{S_{pe}}{S_q} \left( \frac{1}{\bar{C}_{pe}} \right)^2 \quad \text{and} \quad |\chi_{rq}|^2 = \frac{S_{pr}}{S_q} \left( \frac{1}{\bar{C}_{pr}} \right)^2 \quad (27)$$

and need to be determined experimentally together with the phase difference between the external pressures at the opening and the roof  $\phi_{e/r}$ .

The internal and net roof pressure admittance functions, given by Eqs. (25) and (26), are similar to those of a two-degree-of-freedom mechanical system, consisting of two mass-spring-damper systems, being excited by two forces acting on the two masses. Such systems exhibit two resonant modes, the first where the masses oscillate in phase, and the second where the oscillations are 180° out of phase. The corresponding un-damped natural frequencies  $f_1$  and  $f_2$  are obtained by setting the damping terms to zero and then equating the denominator of Eq. (22) to zero, hence

$$f_{1,2} = \left( \frac{1}{2}(f_{HH}^2 + f_r^2 + f_{rp}^2) \mp \left( \left( \frac{1}{2}(f_{HH}^2 + f_r^2 + f_{rp}^2) \right)^2 - f_{HH}^2 f_r^2 \right)^{1/2} \right)^{1/2} \quad (28)$$

It is also possible to derive the admittance function for the roof response over the onset ridge height dynamic pressure ( $S_{xr}$  is the frequency spectrum of roof response  $x_r$ )

$$|\chi_{FR-q}|^2 = \left( \frac{m_r \omega_r^2}{A_r \bar{C}_{pn}} \right)^2 \frac{S_{xr}}{S_q} = \left| \frac{m_r \omega_r^2 x_r}{A_r \bar{C}_{pn} q} \right|^2 = \left( \frac{\bar{C}_{pe}}{\bar{C}_{pn}} \right)^2 |\chi_{nq}|^2 \frac{\omega_r^4}{(\omega_r^2 - \omega^2)^2 + (2\zeta_r \omega_r \omega)^2} \quad (29)$$

The RMS values for the fluctuating internal pressure and roof net pressure coefficients may then be obtained by integration respectively, of the corresponding pressure coefficient spectra

$$\tilde{C}_{pi}^2 = \int_0^\infty S_{C_{pi}}(f) df = \int_0^\infty |\chi_{iq}|^2 (\bar{C}_{pi}/\bar{q})^2 S_q(f) df \quad (30)$$

$$\tilde{C}_{pn}^2 = \int_0^\infty S_{C_{pn}}(f) df = \int_0^\infty |\chi_{nq}|^2 (\bar{C}_{pn}/\bar{q})^2 S_q(f) df \quad (31)$$

### 3. Gain and phase functions $|\chi_{eq}|$ , $|\chi_{rq}|$ and $\phi_{e/r}$

Sharma (2008) measured the functions  $|\chi_{eq}|$ ,  $|\chi_{rq}|$  and  $\phi_{e/r}$  for a wall area equivalent to an opening of full-scale dimensions 2.25 m x 1.25 m, and that for half of the roof of a rectangular 1:50 scale model of low-rise building, as shown in Fig. 3. Full details of the tests and analysis

procedure will be found in Sharma (2008). The results are presented in Figs. 4(a) and (b), which firstly shows, not surprisingly, that the gain functions for the pressures applied at the opening and the roof are attenuated in the high frequency region as discussed in Sharma and Richards (2004).

More interestingly, the phase difference between the two pressures in Fig. 4(b), clearly shows that  $\phi_{e/r} = 180^\circ$  or  $\pi$  radians over most of the frequency range of interest. This simple relationship can easily be implemented in the calculation of the admittance functions.

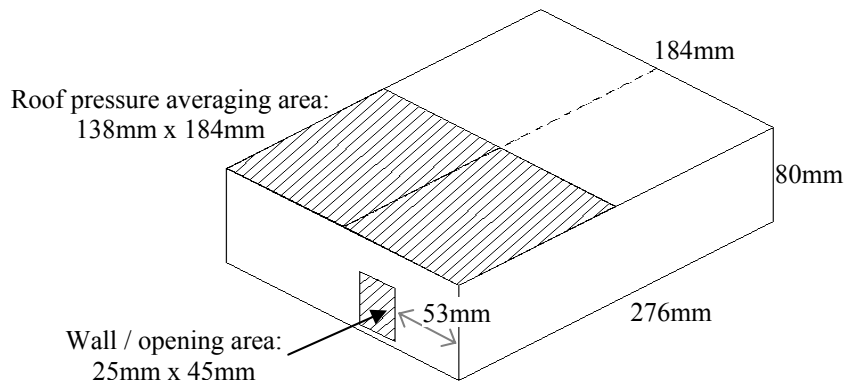


Fig. 3 Model details and pressure averaging areas

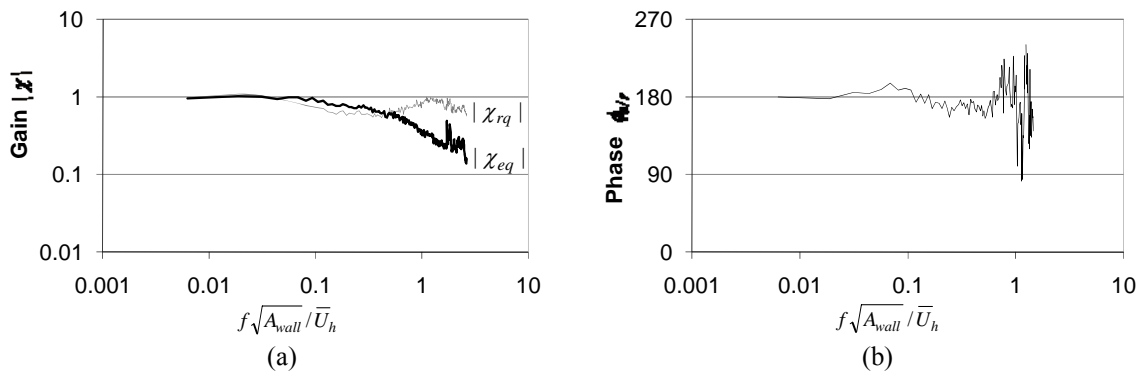


Fig. 4(a) Gain functions  $|\chi_{eq}|$  and  $|\chi_{rq}|$  and (b) Phase difference function  $\phi_{e/r}$

## 4. Analysis, results and discussions

### 4.1 Analysis method

As an example, we consider the same building considered in Sharma (2008) for the quasi-static flexibility analysis

$$\begin{array}{lll}
 \forall_o = 497 \text{ m}^3 & A_o = 2.813 \text{ m}^2 & L_e = \sqrt{\pi A_o} / 4 \\
 c = 0.6 & C_L = 1.2, 2.5, 10, 50 & \\
 \bar{U}_h = 30 \text{ m/s} & I_u = 0.18 & \\
 \rho = 1.22 \text{ kg/m}^3 & \gamma = 1.4 & p_a = 101300 \text{ Pa} \\
 \bar{C}_{pi} = \bar{C}_{pe} = 0.57 & \bar{C}_{pr} = -0.65 & \tilde{C}_{pr} = 0.17 \\
 A_r = 127.1 \text{ m}^2 & m_r = 3500 \text{ kg} & \omega_r = 2\pi f_r, \\
 f_r = 3 \text{ Hz}, 5 \text{ Hz}, 10 \text{ Hz} & \zeta_r = 0.00, 0.05, 0.10, 0.15, 0.20, 0.25 & 
 \end{array}$$

For comparison purposes, it is noted that Sharma (2008) considered quasi-static flexible buildings with the ratio of the bulk modulus of air ( $\gamma p_a$ ) to that of the building ( $k_b$ ),  $b = \gamma p_a / k_b = 0$  for a rigid building, 0.334 and 1.335 for two different flexible buildings. The two non-zero values for  $b$  were estimated by assuming roof structural frequencies  $f_r = 10$  Hz and 5 Hz respectively, with rectangular roof plan area  $A_r = 127.1 \text{ m}^2$  and mass  $m_r = 3500$  kg. In this paper, an additional value of the flexibility parameter  $b = 3.707$  corresponding to  $f_r = 3$  Hz is considered. The building height  $h$  was taken as 4 m, and assumption of vertical roof deflections applied. The building bulk modulus could then be estimated,  $k_b = (2\pi f_r)^2 \forall_o m_r / A_r^2$  or  $b = \omega_{rp}^2 / \omega_r^2$  where  $\omega_{rp} = \sqrt{k_{rp} / m_r}$  and  $k_{rp} = \gamma A_r^2 p_a / \forall_o$  is the pneumatic stiffness of the roof with respect to the contained air.

The internal and combined pressure admittance functions, the roof response admittance functions and the corresponding spectra were calculated using the equations developed in Section 2. The gain functions for the pressures at the opening and the roof  $|\chi_{eq}|$  and  $|\chi_{rq}|$  were taken as those measured in the wind tunnel (see Section 3), with the frequency being scaled to full-scale by preserving the Strouhal number  $f \sqrt{A_{wall}} / \bar{U}_h$ . The measured phase differences  $\phi_{e/r}$  were used for the entire frequency range, scaled to full-scale up to 10 Hz (see Fig. 4(b)). Pressure coefficient spectra were generated from admittances in Fig. 4(a) and the Kaimal turbulence spectrum (Stull 1988)

$$\frac{f S_u(f)}{u_*^2} = \frac{105n}{(1 + 33n)^{5/3}} ; \quad S_{Cq}(f) = \left( \frac{2}{U_z} \right)^2 S_u(f) ; \quad n = \frac{fz}{U_z} \quad (32)$$

with  $z = h = 4$  m. In Eq. (32),  $S_u$  is the spectrum of wind turbulence, while  $S_{Cq} = S_q / \bar{q}^2$  is the spectrum of dynamic pressure coefficient ( $C_q = q / \bar{q}$ ) fluctuations.

#### 4.2 Admittance functions and spectra for internal and net roof pressures

Figs. 5(a) and (b) compare internal and net roof pressure admittance functions respectively for a flexible building ( $f_r = 5$  Hz or  $b = 1.335$ ) obtained from the dynamic flexibility model to those obtained from the quasi-static flexibility and rigid building models. Three roof damping ratios  $\zeta_r = 0.00, 0.10$  and  $0.20$  together with a fixed opening loss coefficient  $C_L = 1.2$ , were used for the dynamic flexibility model calculations. Fig. 5(a) shows that the most significant difference between the dynamic and quasi-static models is in the presence of the second resonance peak in  $|\chi_{iq}|^2$  obtained from the dynamic model. The position of the first resonant peak(s) are however very similar from the two models. These observations also apply to the combined roof pressure admittance functions presented in Fig. 5(b). The two peaks represent two resonant modes; first where the air slug oscillations at the opening are in-phase with roof oscillations; while the higher frequency mode where the air slug oscillations at the opening are anti-phase with roof oscillations. This behaviour is very similar to a two-degree-of-freedom mechanical system.

It should be noted however, that the peak responses from the dynamic model will be dependent on the roof damping ratio  $\zeta_r$ , the effect of which on the admittance functions is illustrated also in Figs. 5(a) and (b). The expected result that with smaller  $\zeta_r = 0.10$  compared to a larger  $\zeta_r = 0.20$ , the peak response is stronger, is shown. In particular, the response at the second resonance appears to be much more sensitive to  $\zeta_r$ . Vickery and Georgiou (1991) in their formulation used  $\zeta_r = 0$  on the assumption that the interactive damping might be dominant. The responses shown here suggest otherwise, although their assumption might be considered to be conservative. However, if the second resonance is in the tail of the onset turbulence spectrum, then using  $\zeta_r = 0$  might not be an unreasonable assumption. Calculation of the RMS responses will shed more light on this.

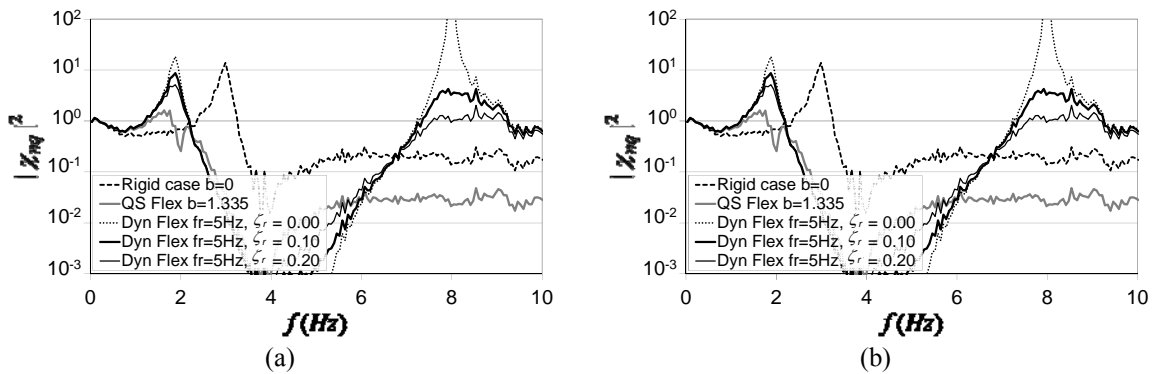


Fig.5 (a) Internal pressure admittance functions (QS Flex = quasi-static flexibility; Dyn Flex = dynamic flexibility) and (b) Net roof pressure admittance functions (QS Flex = quasi-static flexibility; Dyn Flex = dynamic flexibility)

Figs. 6(a) and (b) compare internal and net roof pressure admittance functions respectively obtained from the dynamic flexibility model for a flexible building ( $f_r = 5$  Hz) with a dominant opening, to those obtained: for the case when the influence of roof external pressure fluctuations on internal pressure through the flexible roof are excluded (w/o  $|\chi_{ir}|$ ); and also to those when the

opening is closed off (w/o  $|\chi_{ie}|$  i.e., internal pressure is induced only via the flexible roof). These reveal firstly that a building without a dominant opening but with a flexible roof could induce significant internal pressure fluctuations. The two peaks in the admittances w/o  $|\chi_{ie}|$  correspond to the pneumatic spring mode of the roof – internal air system (natural frequency  $f_{rp}$ ) and the roof structural resonance ( $f_r$ ) modes. Since mean internal pressure is zero for this case, the admittances rapidly fall off towards zero as  $f$  approaches 0. Secondly, the plots show that when the influence of roof external pressure fluctuations on internal pressure via the flexible roof is ignored (shown as w/o  $|\chi_{ir}|$  in Figs. 6(a) and (b)), then the responses that are calculated are very different and likely to lead to erroneous results. Interestingly, previous studies have tended to ignore the contribution of internal pressure generated by transmission through a flexible building envelope.

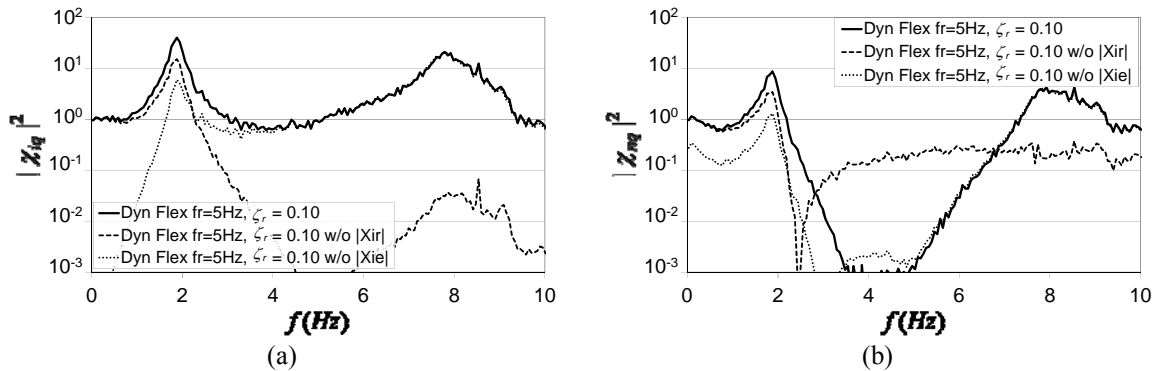


Fig. 6(a) Internal pressure admittance functions (Dyn Flex = dynamic flexibility) and (b) Net roof pressure admittance functions (Dyn Flex = dynamic flexibility)

In Figs. 7(a) and (c), the admittance functions for internal pressure and net roof pressure are compared on the basis of the roof structural natural frequency  $f_r$ . The corresponding admittances obtained using the quasi-static flexibility model are shown in Figs. 7(b) and (d), and which are very different to those from the dynamic flexibility model. In particular, the quasi-static model shows enhanced damping of the resonance, whereas the reduction in response at the first resonance in Figs. 7(a) and (c) are not as severe. The second peak obviously is not captured by the quasi-static flexibility model. Returning to Figs. 7(a) and (c), increasing building flexibility, represented by decreasing values of  $f_r$ , has the effect firstly of decreasing considerably the first resonance frequency  $f_1$ . Secondly, whilst it decreases the peak internal and combined pressure responses at  $f_1$ , it however increases the responses at the second resonance frequency  $f_2$ . The values of  $f_2$  are also reduced, but to a lesser extent than  $f_1$ , since it is limited by the pneumatic stiffness of the roof. These effects are clearly reflected in the internal and net roof pressure coefficient spectra presented in Figs. 8(a) and (b). The significance of the reduction in the natural frequencies, as discussed previously by Sharma (1996) and by Sharma and Richards (1997b), is that the energy available for excitation of the resonance modes is increased for buildings that are more flexible

than those that are less so. This possibly offsets the reduction in response due to the increased damping of the first mode.

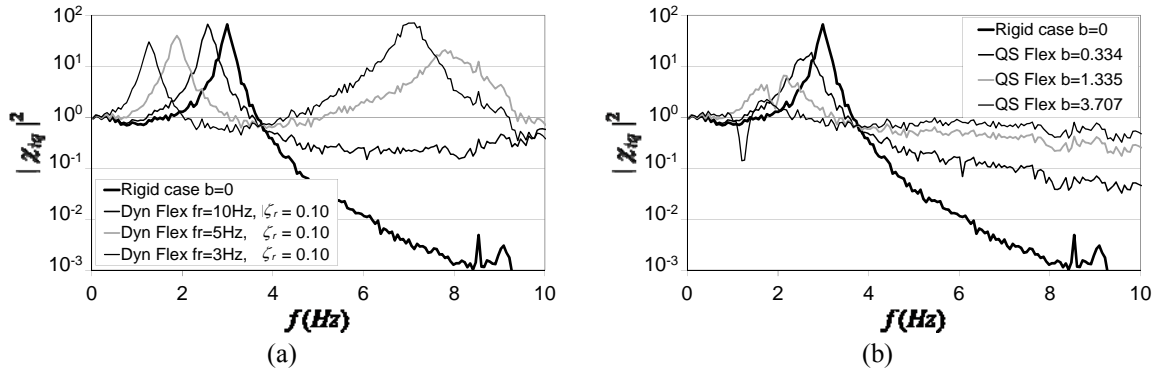


Fig. 7 (a) Internal pressure admittance functions – dynamic flexibility (Dyn Flex) and (b) Internal pressure admittance functions – quasi-static flexibility (QS Flex)

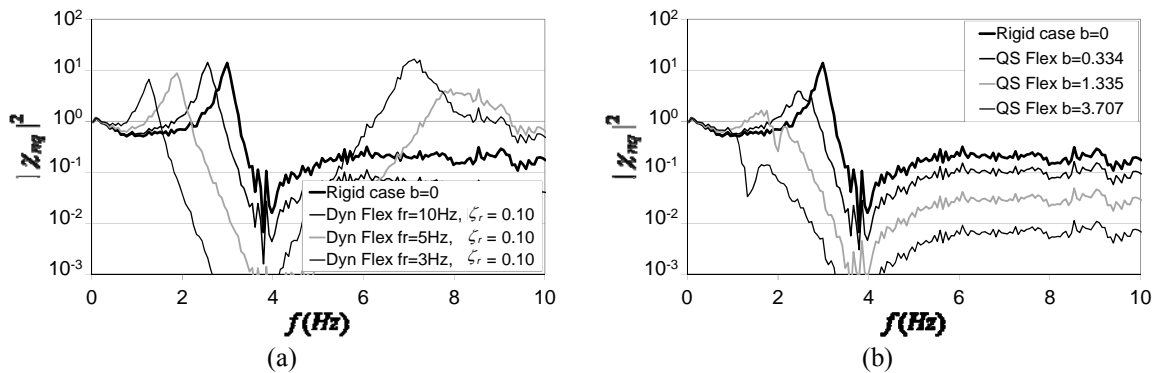


Fig. 7(c) Net roof pressure admittance functions – dynamic flexibility (Dyn Flex) and Net roof pressure admittance functions – quasi-static flexibility (QS Flex)

#### 4.3 RMS pressure coefficients and correlation coefficients – influence of roof flexibility

The RMS pressure coefficients obtained by numerical integration of the respective spectra are presented as functions of the flexibility parameter  $b$  in Figs. 9(a) and (b). The first observation here is that the fluctuations in both internal and roof net pressure, indicated by the RMS coefficients, increase with a dynamically flexible roof. Only when the roof damping ratio  $\zeta_r$  becomes high, to around 0.50, that the fluctuations reduce to the levels for a rigid building case. As previously reported by Sharma (2008) and shown here, a quasi-statically flexible roof effects internal and net roof pressure fluctuations that are reduced relative to the rigid building case. The RMS coefficients decrease with increasing quasi-static flexibility of the roof. Only when the roof damping ratio approaches the critical value  $\zeta_r = 1$ , that the RMS coefficients from the dynamic flexible model approach those for the quasi-static flexibility case. These demonstrate that estimates

of internal and roof net pressure fluctuations from a quasi-static flexibility model are likely to be non conservative when applied to a dynamically flexible building.

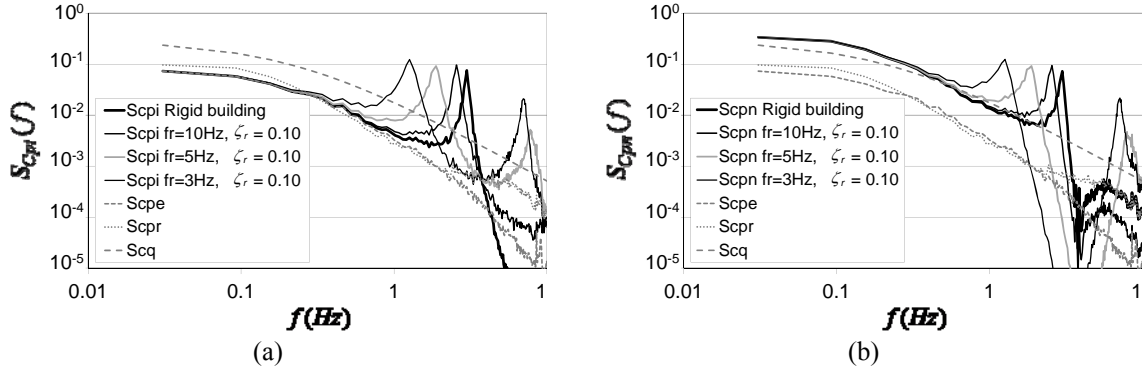


Fig. 8(a) Internal pressure coefficient spectra – dynamic flexibility and (b) Net roof pressure coefficient spectra – dynamic flexibility

The RMS coefficients obtained when the influence of the flexible roof on internal pressure is not included in the calculations, are shown in Figs. 10(a) and 10(b). When compared to the coefficients in Figs 9(a) and (b), these show that the component of internal pressure fluctuations induced via a flexible roof can be significant, even for a quasi-statically flexible roof. The RMS coefficients are therefore a lot different in the comparisons, for example the RMS internal pressure coefficients are seen to decrease in Figure 10a whereas they increase in Fig. 9(a) with building flexibility.

#### 4.4 Influence of roof damping coefficient and opening loss coefficient

A poorly defined and much debated parameter in the building internal pressure dynamic problem is the opening loss coefficient  $C_L$ . Researchers have used, assumed, or determined values ranging from 1.2 (Sharma and Richards 1997a) through 2.5 (Vickery 1994, Oh *et al.* 2007) to 40 (Holmes 1979, Ginger *et al.* 2008). Furthermore, the damping ratio of a flexible roof could range from close to zero  $\zeta_r = 0$  (as assumed by Vickery and Georgiou 1991) to the critical value  $\zeta_r = 1$  (the quasi-static flexibility case). The sensitivity of the results to these parameters was therefore investigated and which are presented in Figs. 11(a) and (b). As might have been expected, the RMS coefficients of internal and net roof pressure fluctuations decrease with increases in both  $\zeta_r$  and  $C_L$ . In the real situation, the values for  $\zeta_r$  and  $C_L$  may be difficult to estimate. Nevertheless, the sensitivity analysis for the building and wind conditions considered here, reveal that  $\tilde{C}_{pi}$  could range from nearly 0.3 when  $\zeta_r$  and  $C_L$  are both low, to approximately the value of the opening external pressure RMS coefficient  $\tilde{C}_{pe}$  when  $C_L$  is high ( $\sim 50$ ). Correspondingly,  $\tilde{C}_{pn}$  varies between 0.4 and 0.27. Note that if  $\tilde{C}_{pi} \approx \tilde{C}_{pe} = 0.15$  were assumed for high values of  $\zeta_r$  and  $C_L$ ,

and since  $\tilde{C}_{pr} = -0.17$ , then if there were (a) 100% correlation (coefficient  $\rho_{ir} = -1.0$ ), and (b) 0% correlation ( $\rho_{ir} = 0$ ), between internal and roof external pressures, then the limiting values for  $\tilde{C}_{pn} = \sqrt{\tilde{C}_{pi}^2 + \tilde{C}_{pr}^2 - 2\rho_{ir}\tilde{C}_{pi}\tilde{C}_{pr}} = 0.32$  and  $0.23$  are obtained, respectively. The lower bound value of  $0.27$  from the dynamic flexibility model calculations lies within this range.

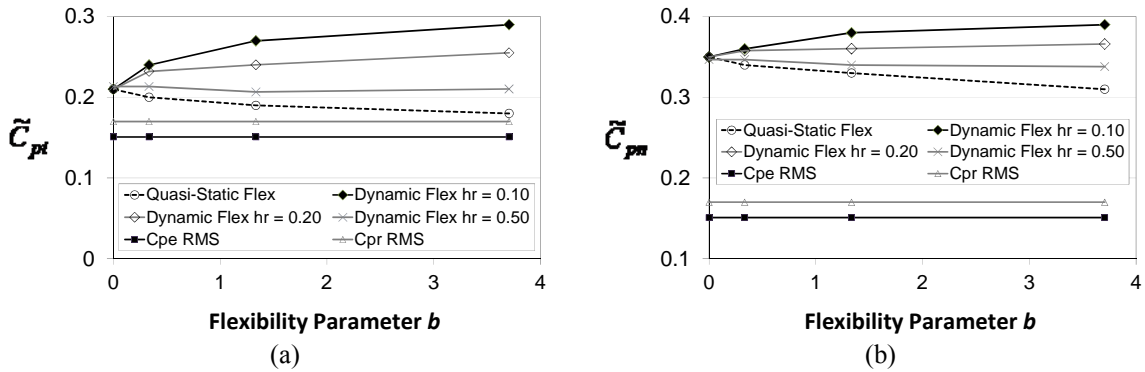


Fig. 9(a) RMS internal pressure coefficients and (b) RMS net roof pressure coefficients

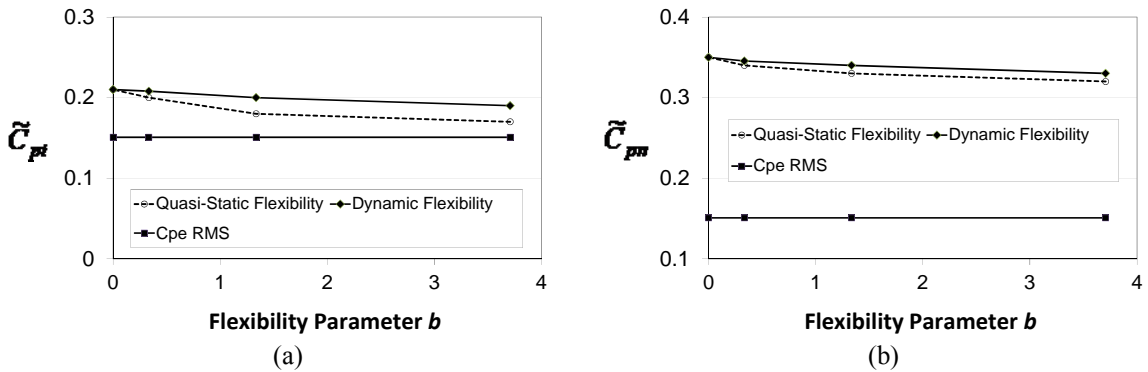


Fig.10 (a) RMS internal pressure coefficients – without  $|\chi_{ir}|$  influence on  $\tilde{C}_{pi}$  and (b) RMS net roof pressure coefficients – without  $|\chi_{ir}|$  influence on  $\tilde{C}_{pi}$

## 5. Experiments

### 5.1 Model details and experimental methodology

With the difficulty associated with modelling a flexible roof on a model building to proper scale and detail, a somewhat simplified cylindrical model was studied in turbulent shear flow generated in the wind tunnel. The model as illustrated in Figure 12, has a cavity volume  $140$  mm diameter by  $247$  mm long ( $V_o = 3.8 \times 10^{-3} \text{ m}^3$ ), with one end having a rubber diaphragm onto

which a 50g Perspex plate is glued (total mass  $m_r = 83\text{g}$  and  $A_r = 1.539 \times 10^{-2} \text{ m}^2$ ). The flexible diaphragm is attached to a clamp that can be pulled over the cylinder so that the flexibility could be varied readily. Since the opposite end of the cylinder is removable, the opening geometry could also be varied relatively easily. Two such configurations were studied over  $0 - 90^\circ$  wind angle range (relative to normal of end containing the opening), the first denoted CYLINDER-1 (CYL-1) with a 25 mm diameter-19 mm long aperture, and second denoted CYLINDER-2 (CYL-2), with a 19 mm diameter-60mm long aperture. The flexibility of the diaphragm was measured by sealing the opening, and then beating the diaphragm as a drum, and the measured internal pressure spectrum displayed a peak at a frequency  $f_R^2 = f_r^2 + f_{rp}^2$ . The diaphragm natural frequency  $f_r$  is then readily obtained since its pneumatic frequency  $f_{rp}$  can be calculated from the expression

$$\omega_{rp} = \sqrt{\gamma A_r^2 p_a / m_r \nabla_o} = 2\pi f_{rp} \text{ included with Eqs. (16) and (17) in Section 2.2.}$$

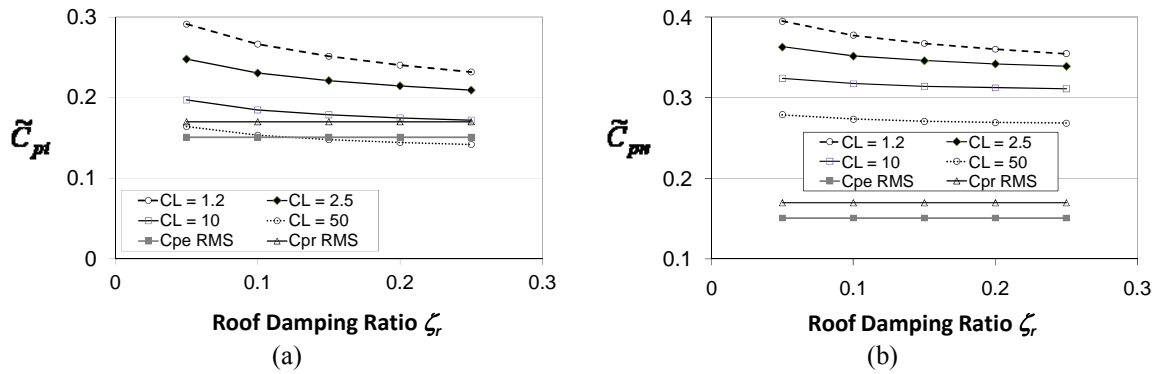


Fig. 11(a) RMS internal pressure coefficient as a function of opening loss coefficient and roof damping and (b) RMS net roof pressure coefficient as a function of opening loss coefficient and roof damping

Internal and external pressure measurements were conducted in a 1:50 scale terrain category 2 (Standards Australia., Standards New Zealand 2002) boundary layer simulation in the de Bray wind tunnel at the University of Auckland. Full characteristics of the boundary layer simulation are described in Sharma and Richards (2005). For both arrangements, the internal pressure to onset mid-opening height dynamic pressure admittance function

$$|\chi_{iq}|^2 = \frac{S_{pi}(f)}{\bar{C}_{pi}^2 S_q(f)} = \frac{S_{pi}(f)}{(\rho U \bar{C}_{pi})^2 S_u(f)} \quad (33)$$

were determined from spectral measurements - the procedure being exactly the same as that described in Sharma and Richards (2004). For CYLINDER-2, the statistics of internal pressure against wind direction were also measured according to the procedure described in Sharma and Richards (2003, 2005).

## 5.2 Results and discussions

Figs. 13(a) and (b) show the admittance functions for CYLINDER-1 at normal  $0^\circ$  and oblique  $50^\circ$  wind respectively. Each plot includes an admittance function for the corresponding rigid cylinder. The results presented here are in qualitative agreement with theory and analytical results examined earlier for the dynamic model. In particular, the first resonance frequency is lowered, and the peak value is decreased due to increased damping. It is interesting to note that for an oblique  $50^\circ$  wind, the phenomenon of Helmholtz resonance under oblique flow is evident, since the admittance peak values are several orders of magnitude higher than for  $0^\circ$  wind. This phenomenon has previously been discussed in detail by Sharma and Richards (2003). This is particularly noticeable for the case of the rigid cylinder.

The flexibility of this cylinder was measured to give  $f_R = \sqrt{f_r^2 + f_{rp}^2} = 111$  Hz, so that a calculated value of  $f_{rp} = 51.4$  Hz means  $f_r = 98.4$  Hz. With a measured (or predicted) Helmholtz frequency  $f_{HH} = 98$  Hz at  $0^\circ$  wind, Eq. (28) yields the two undamped natural frequencies  $f_1 = 77.6$  Hz and  $f_2 = 125.8$  Hz. These compare reasonably with the measured values of 75 Hz and 127 Hz. At  $50^\circ$  wind flow the predicted values of 75.3 Hz and 127.7 Hz also compare well with the measured values of 77 Hz and 127.3 Hz.

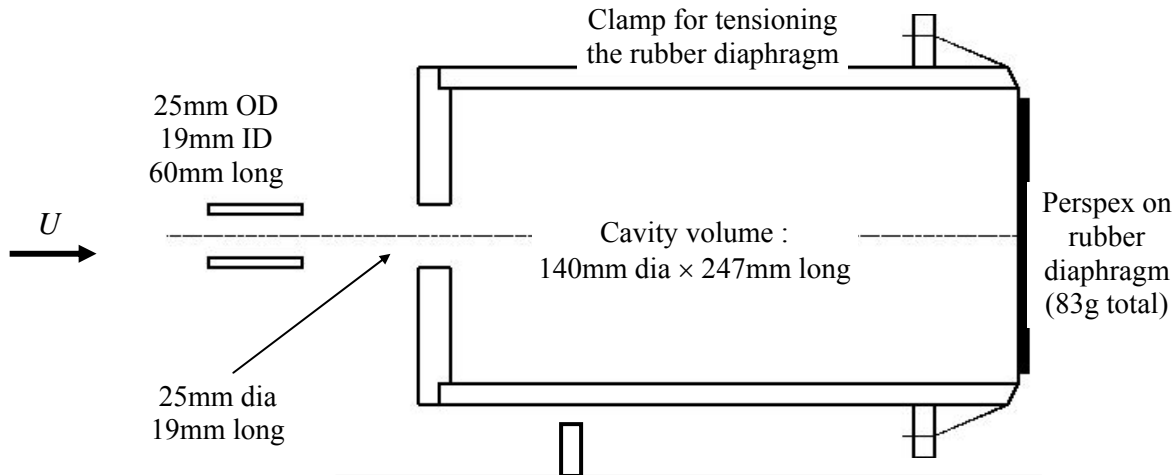


Fig. 12 Details of the flexible cylindrical model

These results are summarised in Table 1, which also shows the RMS values of fluctuating internal pressure coefficient. At  $0^\circ$  wind, the values of  $\tilde{C}_{pi}$  are the same for the rigid and the flexible arrangements of CYLINDER-1. For this particular case therefore, flexibility does not reduce the dynamic component of internal pressure, but maintains it at the same level as that for a rigid case. The reasons for this are not clear cut. However, it might be speculated here that, pressure fluctuations associated with vortex dynamics on the leeward end, where the flexible diaphragm is located, perhaps induces strong internal pressures fluctuations via the flexible diaphragm. This situation is significantly different to a flexible roof where vortex dynamics may

not be present. On the other hand at 50° wind, a considerable reduction is observed in the value of  $\tilde{C}_{pi}$  for the flexible case over the rigid case. This corroborates the deductions from the analytical model developed earlier.

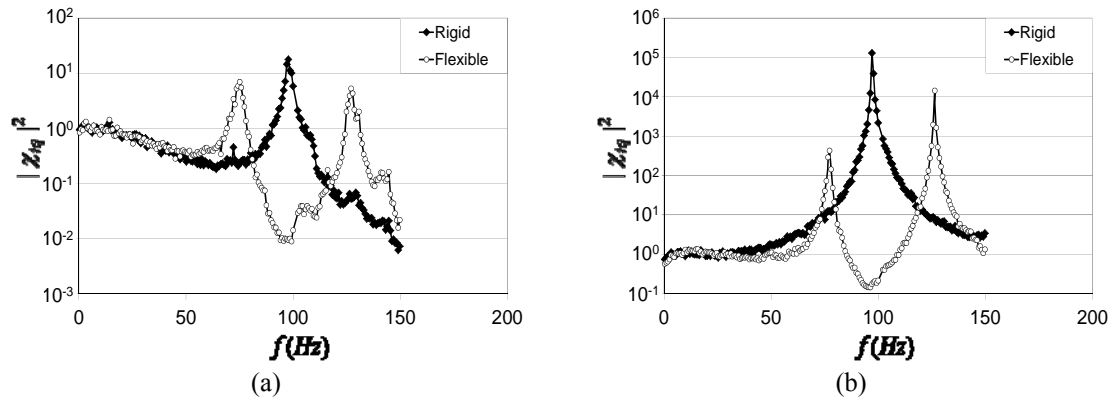


Fig. 13(a) Internal pressure admittance functions for CYLINDER-1 at 0° wind and  
 (b) Internal pressure admittance functions for CYLINDER-1 at 50° wind

Table 1 Natural frequencies and RMS internal pressure coefficients for the two cylinders

	$f_{HH}$	$f_r$	$f_{rp}$	$f_1$ (Hz)		$f_2$ (Hz)		$\tilde{C}_{pi}$	
	(Hz)	(Hz)	(Hz)	Pred'n	Meas'd	Pred'n	Meas'd	Rigid	Flex
CYL-1 0°	98	98.4	51.4	76.6	75	125.8	127	0.21	0.21
CYL-1 50°	97	98.4	51.4	75.3	77	126.7	126.3	1.22	0.35
CYL-2 0°	53	58.7	51.4	35.6	33.5	87.3	83	0.23	0.25
CYL-2 80°	54	58.7	51.4	36.1	36	87.7	85	0.52	0.29

The admittance functions for CYLINDER-2 are plotted in Figs. 14(a) and (b) which generally show the same trends observed for CYLINDER-1. While in general, the predicted values of the natural frequencies agree fairly well with the measured values, for normal 0° wind however, the second resonance which is much weaker, occurs at 83 Hz rather than closer to the predicted frequency of 87.3 Hz; see Table 1. Another similar peak occurs at just over 100 Hz, which might be associated with vortex shedding effects at the rear of the cylinder. Since the second resonance is not strong, it is believed that the model is not flexible enough, and therefore displays a quasi-static type of behaviour. A slight increase is observed in the value of  $\tilde{C}_{pi}$  at normal 0° wind, for the flexible case as compared to the rigid case. The comments made for CYLINDER-1 regarding the response under oblique flow are also applicable to this cylinder.

The variation of internal pressure coefficients for CYLINDER-2 with wind direction are plotted in Figures 15a and 15b. The peak-ratios (i.e., ratio of peak pressure to peak dynamic pressure)  $C_{\hat{p}/\hat{q}} = \hat{p}/\hat{q} = \hat{p}/\frac{1}{2}\rho_a\hat{U}_h^2$  (see Sharma and Richards 2003) are consistently higher in magnitude

than the mean internal pressure coefficient  $\bar{C}_{pi}$  at all wind flow angles. As discussed by Sharma and Richards (2003), peak-ratio is a good indicator of the influence of phenomena such as Helmholtz resonance, due to which the quasi-steady assumption ( $C_{\hat{p}i/\hat{q}} = \bar{C}_{pi}$ ) breaks down, that is  $C_{\hat{p}i/\hat{q}} \neq \bar{C}_{pi}$ . Of note in the context of discussions on the effects of flexibility are:

(a) Over the 0-60° wind angle range, the values of  $C_{\hat{p}i/\hat{q}}$  and the RMS coefficients  $\tilde{C}_{pi}$  from the flexible model are very similar to those obtained for the rigid model. This might appear to be an unexpected result from the viewpoint of the analysis of Section 4. However, it is noted that the flexible diaphragm is located at the leeward end of the cylindrical model. It is very likely that vortex shedding at the leeward end has considerable influence on the flexible diaphragm (as discussed already) and therefore on the internal pressure.

(b) Beyond a 60° wind, several significant observations are made. First, the values of  $\tilde{C}_{pi}$  are considerably larger for both the rigid and flexible models, compared to the corresponding values over smaller wind angles. Second, the external RMS pressure coefficients  $\tilde{C}_{pe}$  over this range are also enhanced, peaking at a wind angle of around 75°, most probably arising from separation vortex dynamics. Thirdly, the level of enhancement in fluctuations in internal pressure is clarified when the RMS coefficient ratios  $\tilde{C}_{pi} / \tilde{C}_{pe}$  are examined in Fig. 15(c). This shows that the ratios over this range are much larger than those at wind angles lower than 60°, therefore the enhancement in  $\tilde{C}_{pe}$  alone cannot be responsible for this. A more probable explanation is that intense Helmholtz resonance under oblique flow effects are at play, as discussed already. Fourthly, which is more important in the context of this paper, the magnitudes of  $C_{\hat{p}i/\hat{q}}$  and  $\tilde{C}_{pi}$  for the flexible cylinder model are significantly smaller than the corresponding values obtained from the rigid cylinder model. Again, this corroborates the findings from the analysis of Section 4: envelope flexibility reduces fluctuations in internal pressure.

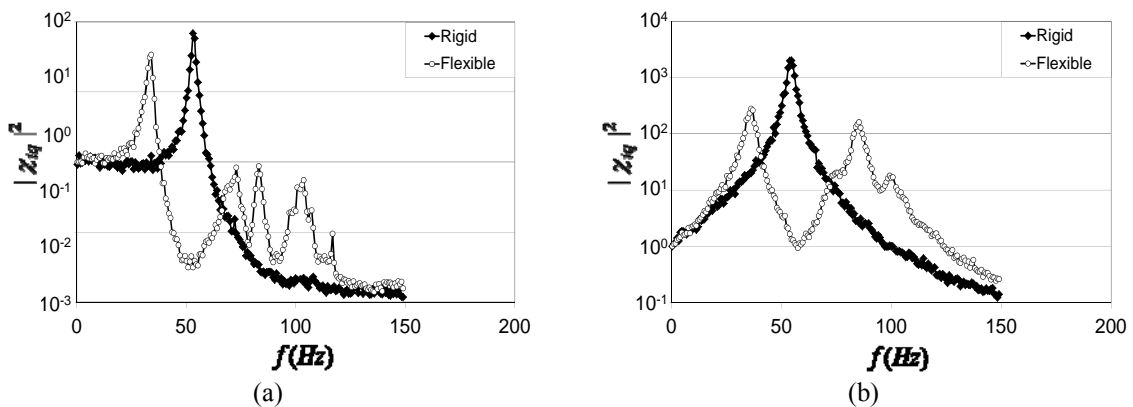


Fig. 14(a) Internal pressure admittance functions for CYLINDER-2 at 0° wind and  
 (b) Internal pressure admittance functions for CYLINDER-2 at 80° wind

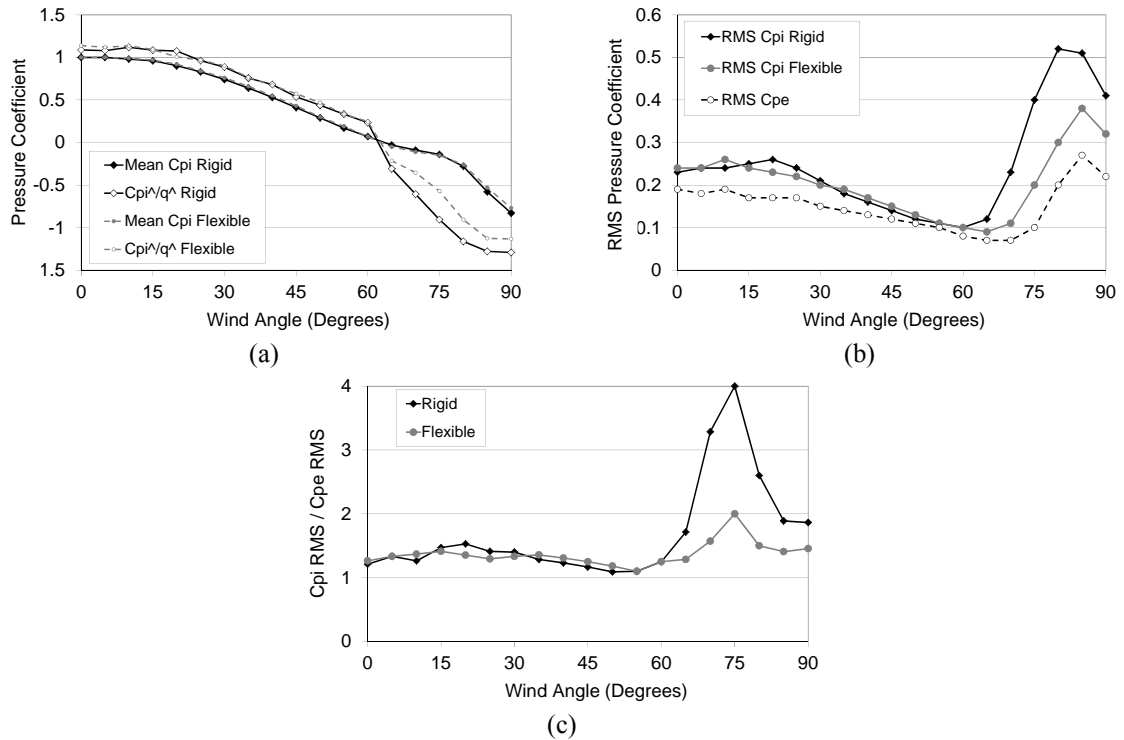


Fig. 15(a) Mean and peak-ratio internal pressure coefficients for CYLINDER-2, (b) RMS internal pressure coefficients for CYLINDER-2 and (c) Ratio of RMS pressure coefficients for CYLINDER-2

## 6. Conclusions

An analytical model has been developed for internal and net envelope pressures acting on a building having dynamic envelope flexibility and a dominant opening. Linearised equations were also obtained for the case where an envelope, for example the roof, responds in a dynamic manner. Equations describing the admittance functions for internal pressure, net roof pressure and the roof responses have also been obtained. It is shown that dynamic interaction between the flexible roof and the internal pressure results in a coupled system that is similar to a two-degree-of-freedom mechanical system consisting of two mass-spring-damper systems with excitation forces acting on both the masses. Two resonant modes are present, the natural frequencies of which can readily be obtained from the model. These are dependent upon the Helmholtz frequency of the corresponding rigid building cavity, the roof structural natural frequency and the frequency associated with the pneumatic stiffness of the roof.

As observed for the case of increasing quasi-static building flexibility, the effect of increased dynamic flexibility is to reduce the first natural frequency as well as the corresponding peak value of the admittance, the latter being the result of increased damping effects of building flexibility. Consequently, it is found that the internal and net roof pressure fluctuations (RMS coefficients) are also reduced with dynamic flexibility. Some experiments conducted using a cylindrical model

(with a leeward end flexible diaphragm) provides validity to this model via good match between predicted and measured natural frequencies, reduction in peak admittance with the flexible model relative to those of the rigid model, and significant reductions in RMS response with flexibility.

It is also found that significant differences exist between internal and net roof pressure responses obtained from the dynamic flexibility model, and those obtained from the quasi-static flexibility model. Hence it is concluded that the quasi-static assumption should be applied with care, and is not applicable to dynamically flexible buildings.

Furthermore, sensitivity analyses have revealed that the responses are sensitive to both the opening loss coefficient and the roof damping ratio. Careful estimates should therefore be made to opening loss coefficients first, if the predictions from such models are to have significance to real buildings.

## Acknowledgements

The financial support of the University of the South Pacific, Suva, Fiji Islands and the New Zealand Government are gratefully acknowledged.

## References

- American Society of Civil Engineers (ASCE). (2005), *ASCE 7-05 - Minimum Design Loads for Buildings and Other Structures, Part 6: Wind loads. ASCE/SEI 2005*.
- Ginger, J.D., Holmes, J.D., and Kopp, G.A. (2008), "Effect of building volume and opening size on fluctuating internal pressure", *Wind Struct.*, **11**(5), 361-376.
- Guha, T.K., Sharma, R.N. and Richards, P.J. (2012), "Internal pressure dynamics of a leaky and quasi-statically flexible building with a dominant opening", accepted for publication in *Wind Struct.*
- Holmes, J.D. (1980), "Mean and fluctuating pressures induced by wind", *Proceedings of the 5th International Conference on Wind Engineering*, Colorado State University 1979, Pergamon, Oxford.
- Hoxey, R.P. and Richards, P.J. (1995), "Full-scale wind load measurements point the way forward", *J. Wind Eng. Ind. Aerod.*, **57**(2-3), 215-224.
- Liu, H. and Saathoff, P.J. (1981), "Building internal pressure: sudden change", *J. Eng. Mech. - ASCE* **107**(2), 309-321.
- Novak, M. and Kassem, M. (1990), "Effect of acoustical damping on free vibration of light roofs backed by cavities", *J. Wind Eng. Ind. Aerod.*, **36**(1), 289-300.
- Oh, J.H., Kopp, G.A. and Inçulek, D.R. (2007), "The UWO contribution to the NIST aerodynamic database for wind loads on low buildings: Part 3. internal pressures", *J. Wind Eng. Ind. Aerod.*, **29**, 293-302.
- Pearce, W. and Sykes, D.M. (1999), "Wind tunnel measurements of cavity pressure dynamics in a low-rise flexible roofed building", *J. Wind Eng. Ind. Aerod.*, **82**(1-3), 27-48.
- Robertson, A.P. (1992), "The wind-induced response of a full-scale portal framed building", *J. Wind Eng. Ind. Aerod.*, **41-44**, 1677-1688.
- Sharma, R.N. (2011), "Internal pressures in single compartment and partitioned two-compartment buildings with a dominant opening", IN REVIEW, *J. Wind Eng. Ind. Aerod.*
- Sharma, R.N. (2008), "Internal and net envelope pressures in a building having quasi-static flexibility and a dominant opening", *J. Wind Eng. Ind. Aerod.*, **96**(6-7), 1074-1083.
- Sharma, R.N. (2003), "Internal pressure dynamics with internal partitioning", *Proceedings of the 11th International Conf. on Wind Engineering*, Texas Tech University, Lubbock Texas, June.
- Sharma, R.N. (1996), *The influence of internal pressure on wind loading under tropical cyclone conditions*. PhD Thesis in Mechanical Engineering, The University of Auckland.

- Sharma, R.N., Mason, S. and Driver, P. (2010), "Scaling methods for wind tunnel modelling of building internal pressures induced through openings", *Wind Struct.*, **13**(4), 363-374.
- Sharma, R.N. and Richards, P.J. (2005), "Net pressures on the roof of a low-rise building with wall openings", *J. Wind Eng. Ind. Aerod.*, **93**(4), 267-291.
- Sharma, R.N. and Richards, P.J. (2004), "The multi-stage process of windward wall pressure admittance", *J. Wind Eng. Ind. Aerod.*, **92**(14-15), 1191-1218.
- Sharma, R.N. and Richards, P.J. (2003), "The influence of helmholtz resonance on internal pressures in a low-rise building", *J. Wind Eng. Ind. Aerod.*, **91**(6), 807-828.
- Sharma, R.N. and Richards, P.J. (1997a), "Computational modelling of the transient response of building internal pressure to a sudden opening", *J. Wind Eng. Ind. Aerod.*, **72** (1-3), 149-161.
- Sharma, R.N. and Richards, P.J. (1997b), "The effect of roof flexibility on internal pressure fluctuations", *J. Wind Eng. Ind. Aerod.*, **72**, 175-186.
- Standards Australia and Standards New Zealand. (2002), *AS/NZS 1170.2:2002 Structural design actions Part 2: Wind actions*.
- Stull, R.D. (1988), *An Introduction To Boundary Layer Meteorology*, Atmospheric Sciences Library, Kluwer Academic Publishers, The Netherlands.
- Vickery, B.J. (1994), "Internal pressures and interactions with the building envelope", *J. Wind Eng. Ind. Aerod.*, **53**(1-2), 125-144.
- Vickery, B.J. (1986), "Gust factors for internal-pressures in low-rise buildings", *J. Wind Eng. Ind. Aerod.*, **23**, 259-271.
- Vickery, B.J. and Bloxham, C. (1992), "Internal pressure dynamics with a dominant opening", *J. Wind Eng. Ind. Aerod.*, **41**, 193-204.
- Vickery, B.J. and Georgiou, P.N. (1991), "A simplified approach to the determination of the influence of internal pressures on the dynamics of large span roofs", *J. Wind Eng. Ind. Aerod.*, **38**(2-3), 357-369.